International Journal of Enhanced Research in Science, Technology & Engineering
ISSN: 2319-7463, Vol. 5 Issue 5, May-2016

Blind Interference Cancellation Using the Fractional Fourier Transform

Seema Sud

The Aerospace Corporation, Communications and Signal Analysis Dept., VA, USA[1]

ABSTRACT

This paper presents a new method based on the relation of the Fractional Fourier Transform (FrFT) to the Wigner Distribution (WD) to blindly remove interference to recover a signal-of-interest (SOI) in non-stationary environments. Since the SOI and interference may be completely separable by filtering along the optimum FrFT axis, 't_a', we can obtain performance similar to training mode, with moderate E_b/N_0 of 7 to 10 dB, and carrier-to-interference ratios (CIR) of just -2 to 0 dB.

Keywords: Blind adaptive filtering, Fractional Fourier Transform, interference cancellation, mean-square error, Wigner distribution.

1. INTRODUCTION

The Fractional Fourier Transform (FrFT) is a tool for separating non-stationary signals [6]. The FrFT enables us to translate a received signal to an axis in the time-frequency plane where the signal-of-interest (SOI) and interference may be separable [1], when they are not separable in the frequency domain, as produced by the conventional Fast Fourier transform (FFT), or in the time domain.

When applying the FrFT to perform interference suppression (IS), we must first estimate the rotational parameter 'a', $0 \leqslant a \leqslant 2$. Conventional methods choose the 'a' that produces the minimum mean-square error (MMSE) between a desired training signal and its estimate [7]. However, MMSE-FrFT estimation fails in non-stationary environments. FFT-based methods also fail when signals overlap in frequency. Recently, a method was proposed that uses the FrFT's relation to the Wigner Distribution (WD) to optimally compute 'a' using a training sequence and do IS using a reduced rank multistage Wiener filter (MWF) [8]. This technique was shown to provide great improvement in IS over MMSE-FrFT methods even at low signal-to-noise ratio (SNR).

This paper is organized as follows: Section 2 briefly describes the FrFT and WD relationship. Section 3 describes the adaptive filtering problem, now in the Fractional Fourier Transform (FrFT) domain. Section 4 presents the WD-FrFT solution presented in [8] for obtaining 'a' and filtering out the interference. Section 5 describes the proposed modification to the WD-FrFT algorithm when no training data is available. Section 6 has simulation results showing the performance of the proposed blind method compared to the original training-based approach. Finally, a conclusion and remarks on future work are given in Section 7.

2. BACKGROUND: FRACTIONAL FOURIER TRANSFORM (FRFT) AND WIGNER DISTRIBUTION (WD)

The $N \times 1$ FrFT of an $N \times 1$ discrete vector $\mathbf{x}$ is

$$\mathbf{X}_a = \mathbf{F}^a \mathbf{x}, \tag{1}$$

where $\mathbf{F}^a$ is an $N \times N$ matrix whose elements are given by ([2] and [6])

$$\mathbf{F}^a[m,n] = \sum_{k=0,k\neq(N-1+(N)_2)}^{N} u_k[m] e^{-j\frac{\pi}{2}ka} u_k[n], \tag{2}$$

[1]The author gratefully thanks The Aerospace Corporation for funding this work.

and where $u_k[m]$ and $u_k[n]$ are the eigenvectors of the matrix **S** defined by [2]

$$\mathbf{S} = \begin{bmatrix} C_0 & 1 & 0 & \dots & 1 \\ 1 & C_1 & 1 & \dots & 0 \\ 0 & 1 & C_2 & \dots & 0 \\ \vdots & \vdots & \vdots & \ddots & \vdots \\ 1 & 0 & 0 & \dots & C_{N-1} \end{bmatrix}, \tag{3}$$

and

$$C_n = 2cos(\frac{2\pi}{N}n) - 4. \tag{4}$$

The WD is a time-frequency representation of a signal, and may be viewed as a generalization of the Fourier Transform, which is solely the frequency representation. The WD of a discrete signal x[n] can be written as [5]

$$W_x[\frac{n}{2f_s}, \frac{kf_s}{2N}] = e^{j\frac{\pi}{N}kn} \sum_{m=l_1}^{l_2} x[m]x^*[n-m]e^{j\frac{2\pi}{N}km}, \tag{5}$$

where $l_1 = \max(0,n-(N-1))$ and $l_2 = \min(n,N-1)$. A useful property of the FrFT is that the projection of the WD of a signal x(t) onto an axis t_a gives the energy of the signal in the FrFT domain ‘a’, $|\mathbf{X}_a(t)|^2$ (see e.g. [3] or [4]).
The WD of a signal and interference, shown in Fig. 1, illustrates how the FrFT may be used to improve interference cancellation. In non-stationary environments, both the SOI x(t) and the interference $x_I(t)$ vary as a function of time and frequency. The WD shows how they both independently vary. Note that they both overlap in the time domain ($t_{a=0}$) and in the frequency domain ($t_{a=1}$), but there is some axis t_a, $0 < a < 2$, where they do not overlap. If we can find this optimum axis and rotate to it using the FrFT, we can filter out the interference in the new domain and achieve significant IS improvements over conventional time (e.g. MMSE) or frequency (e.g. FFT) filtering.

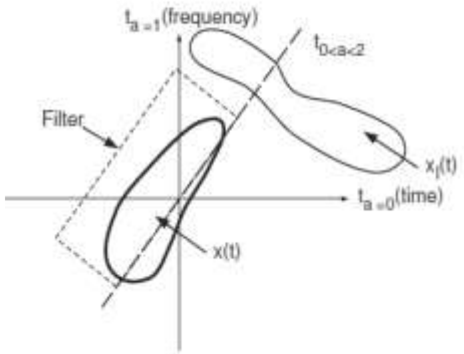

Fig.1: Wigner Distribution of Signal x(t) and Interference $x_I(t)$ Shows Optimum Axis t_a Where Interference May Be Completely Filtered Out

3. PROBLEM FORMULATION

Following [8], we let the SOI be a baseband binary signal denoted as **x**(i), the interferer as $\mathbf{x}_I(i)$, which we will give examples of in Section 6, and noise as an AWGN signal **n**(i). Here, index i denotes the i[th] sample, where i = 1, 2,…, N, and N is the total number of samples per block that we process. The received signal **y**(i) is then

$$\mathbf{y}(i) = \mathbf{x}(i) + \mathbf{x}_I(i) + \mathbf{n}(i). \tag{6}$$

We obtain an estimate of the transmitted signal **x**(i), denoted $\hat{\mathbf{x}}(i)$, by first transforming the received signal to the FrFT domain, applying an adaptive filter, and taking the inverse FrFT. This is written as [7]

$$\hat{\mathbf{x}}(i) = \mathbf{F}^{-a}\mathbf{G}\mathbf{F}^{a}\mathbf{y}(i), \tag{7}$$

where $\mathbf{F}^a$ and $\mathbf{F}^{-a}$ are the N × N FrFT and inverse FrFT matrices of order ‘a’, respectively, and

$$\mathbf{g} = diag(\mathbf{G}) = (g_0, g_1, g_{N-1}) \tag{8}$$

is an N × 1 set of filter coefficients to be found. The notation diag(**G**) = (g_0,g_1,g_{N-1}) means that matrix **G** has the scalar coefficients g_0, g_1,..., and g_{N-1} as its diagonal elements, and all other elements are zero. The goal, therefore, is to first determine the best rotational parameter ‘a’, and then to determine the set of optimum filter coefficients $\mathbf{g}_0$ for cancelling out the interference.

4. METHOD FOR ESTIMATING ‘a’ USING THE RELATION BETWEEN THE FRFT AND THE WD

The algorithm in [8] computes the energy of the FrFT of the SOI and interference, computes their product, sums the values over the new time-frequency axis t_a defined by the rotational parameter ‘a’, and selects as the optimum ‘a’ the value for which the result is minimum. Hence, we minimize [8]

$$\Re_{\mathbf{XX}_I}(a) \equiv \sum_{i=1}^{N} |\mathbf{X}_a(i)|^2 |\mathbf{X}_{I_a}(i)|^2 . \tag{9}$$

This algorithm requires a training sequence **x**(i) to compute $\mathbf{X}_a$(i). This could be, for example, pilots in an orthogonal frequency division multiplexing (OFDM) signal or preambles in a time division multiple access (TDMA) frame. It also uses gaps in the signal, e.g. empty carriers in OFDM or empty slots in TDMA, to estimate $\mathbf{X}_{Ia}$(i). Once we have the best ‘a’, we compute the filter coefficients $\mathbf{g}_0$ from Eq. (14) of [8] using the correlations subtraction architecture of the reduced rank multistage Wiener filter (CSA-MWF) [8]. Those details are given in [8] but are omitted here because we wish to instead study how to estimate ‘a’ blindly. This is discussed next.

5. PROPOSED BLIND METHOD

In the absence of training data **x**(i), we would like to determine how to operate the above algorithm blindly. We propose to do this by replacing **x**(i) with **y**(i), while still using some knowledge about when the SOI is turned off to estimate the interference. Hence, we simply replace **x**(i) with **y**(i) and replace $\mathbf{X}_a$(i) with $\mathbf{Y}_a$(i). The new term to be minimized is then

$$\Re_{\mathbf{YX}_I}(a) \equiv \sum_{i=1}^{N} |\mathbf{Y}_a(i)|^2 |\mathbf{X}_{I_a}(i)|^2 . \tag{10}$$

We can still achieve good performance because this still equates to minimizing $\Re_{XX_I}(a)$. To see this, we write

$$|\mathbf{Y}_a(i)|^2 |\mathbf{X}_{I_a}(i)|^2 = |\mathbf{F}^a \mathbf{y}(i)|^2 |\mathbf{X}_{I_a}(i)|^2 . \tag{11}$$

Using the relationship $|A|^2 = AA^*$, with $*$ denoting complex conjugate, we write

$$= \mathbf{F}^a \mathbf{y}(i) \mathbf{y}^*(i) (\mathbf{F}^a)^* |\mathbf{X}_{I_a}(i)|^2 . \tag{12}$$

Substituting for **y**(i) using Eq. (6),

$$= \mathbf{F}^a (\mathbf{x}(i) + \mathbf{x}_I(i) + \mathbf{n}(i))(\mathbf{x}^*(i) + \mathbf{x}_I^*(i) + \mathbf{n}^*(i))(\mathbf{F}^a)^* |\mathbf{X}_{I_a}(i)|^2 . \tag{13}$$

Assuming the three signals are uncorrelated with each other, thereby eliminating cross-terms, we can expand this to write

$$= (\mathbf{F}^a \mathbf{x}(i) \mathbf{x}^*(i) (\mathbf{F}^a)^* + \mathbf{F}^a \mathbf{x}_I(i) \mathbf{x}_I^*(i) (\mathbf{F}^a)^* \cdot \mathbf{F}^a \mathbf{n}(i) \mathbf{n}^*(i) (\mathbf{F}^a)^*) |\mathbf{X}_{I_a}(i)|^2 \tag{14}$$

$$= (|\mathbf{X}_a(i)|^2 + |\mathbf{X}_{\mathbf{I}a}(i)|^2 + |\mathbf{N}_a(i)|^2) |\mathbf{X}_{I_a}(i)|^2 , \tag{15}$$

where $\mathbf{N}_a$(i) is similarly the FrFT of the noise process. Multiplying out and substituting into Eq. (10), we obtain

$$\Re_{\mathbf{YX}_I}(a) = \Re_{\mathbf{XX}_I}(a) + \Re_{\mathbf{X}_I \mathbf{X}_I}(a) + \Re_{\mathbf{NX}_I}(a), \tag{16}$$

giving the desired result. This expression shows how blind mode incurs performance loss over training mode, due to the presence of the second and third terms in the above equation. Since these terms depend upon noise and interference, we expect the performance loss to be worse as the strength of either increases. We study this loss by simulation in the next section. The new blind mode algorithm is summarized below:

(1) Initialize: $a = 0$.
(2) Compute $|\mathbf{Y}_a(i)|^2 = |\mathbf{F}^a \mathbf{y}(i)|^2$,
(3) Compute $|\mathbf{X_I}_a(i)|^2 = |\mathbf{F}^a \mathbf{x}_I(i)|^2$,
(4) Compute $\Re_{\mathbf{YX}_I}(a) \equiv \sum_{i=1}^{N} |\mathbf{Y}_a(i)|^2 |\mathbf{X}_{I\,a}(i)|^2$.
(5) Increment a and repeat Steps 2 to 4 until $a = 2$.
(6) Choose the value of a for which $\Re_{\mathbf{YX}_I}(a)$ in Step 4 above, is minimum.

Filtering is then performed as before [8].

6. SIMULATIONS

We present simulation examples to compare the proposed WD-FrFT method for calculating the optimum FrFT rotational parameter 'a' blindly vs non-blindly. Then, using the best 'a', we filter with the CSA-MWF and obtain bit estimates. We vary the strength of the interfering signal by setting its amplitude based upon a desired carrier-to-interference ratio (CIR), and we set the amplitude of the AWGN based upon a desired E_b/N_0. We run let N = 2 and run M = 1,000 trials, to obtain histograms of the error between the true bit and its estimate, ϵ , defined by

$$\epsilon = \sqrt{\sum_{i=1}^{N} (\mathbf{x}(i) - \hat{\mathbf{x}}(i))^2 / N}. \tag{17}$$

In the first example, we let the interfering signal take on the form of a chirp signal, given by

$$\mathbf{x}_I(i) = e^{-j1.73\pi (i/f_s)^2}. \tag{18}$$

We set CIR = 0 dB, so the interference is nearly equal in power with the SOI, and we let E_b/N_0 = 10 dB. We sample the data at $f_s = 2R_b$, where the bit rate is R_b = 1 kbps. We increment a, from 0 to 2, using a step size of $\Delta a = 0.01$. A plot comparing the histograms of the mean-square error of the original algorithm in [8] and the proposed blind algorithm is shown in Fig. 2. Averaging over the 1,000 trials gives the means and variances of the error signal as follows: $\mu_{WD-FrFT}$ = 0.2473, $\mu_{WD-FrFT,Blind}$ = 0.2714, $\sigma^2_{WD-FrFT}$ = 0.0076, and $\sigma^2_{WD-FrFT,Blind}$ = 0.0078. Here, we see that due to the presence of noise and interference, the error is slightly worse in blind mode than training mode.

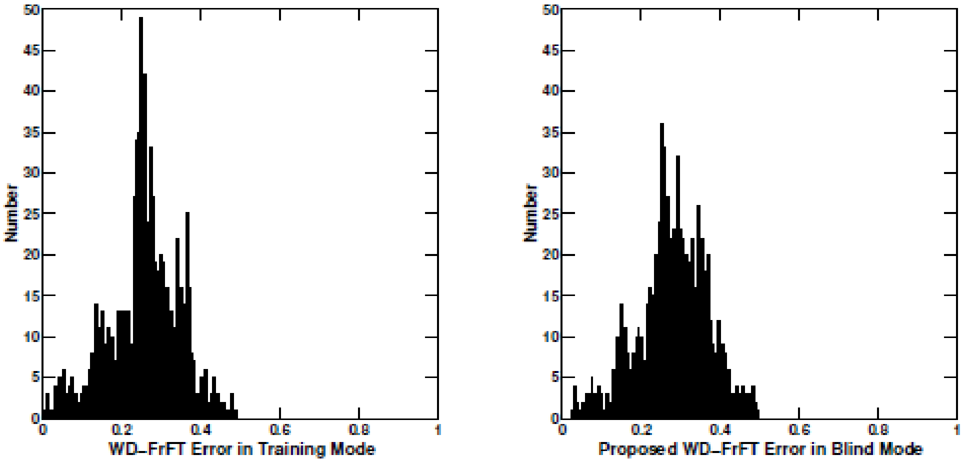

Figure 2. Error with Chirp Interferer, CIR = 0 dB, E_b/N_0 = 10 dB

The second example uses an interfering signal taking on the form of a Gaussian pulse, given by

$$\mathbf{x}_I(i) = \beta e^{-\pi (i/f_s - \phi)^2}, \tag{19}$$

where β and ϕ are the amplitude and phase of the pulse, respectively, uniformly distributed in (1,1.5). All other parameters are the same as in the previous example, e.g. we again let CIR = 0 dB and E_b/N_0 = 10 dB. A plot comparing the histograms of the mean-square error of the three techniques is shown in Fig. 3, where $\mu_{WD-FrFT} = 0.1931$, $\mu_{WD-FrFT,Blind} = 0.2576$, $\sigma^2_{WD-FrFT} = 0.0055$, and $\sigma^2_{WD-FrFT,Blind} = 0.0092$. Again, we notice a small but not significant degradation in blind mode. Note that the performance with both types of interference is similar.

To determine where the blind mode algorithm starts to degrade, we plot the lowest E_b/N_0 we can have as a function of CIR before the blind mode error mean increases by more than 30% over that of training mode. This is shown in Fig. 4, using the Gaussian pulse as the interferer (similar performance is obtained with the chirp interferer). From this plot, we see that the performance is more noise limited than interference limited. This is likely due to the fact that the third term in Eq. (16), based on $|\mathbf{N}_a(i)|^2$, biases the term we are minimizing by the noise power at each sample i, which is stationary and which we cannot estimate. Noise also cannot be completely filtered by the FrFT, as it is uniformly distributed across time and frequency. The non-stationary interference, however, can be better suppressed, and therefore we can operate at CIR down to 0 dB if $E_b/N_0 > 7$ dB. We can even operate at CIR < −2 dB, but this requires $E_b/N_0 > 10$ dB.

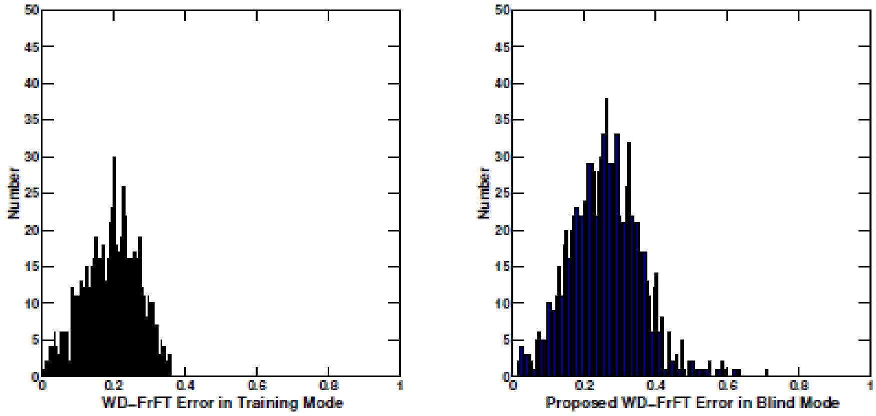

Figure 3. Error with Gaussian Pulse Interferer, CIR = 0 dB, E_b/N_0 = 10 dB

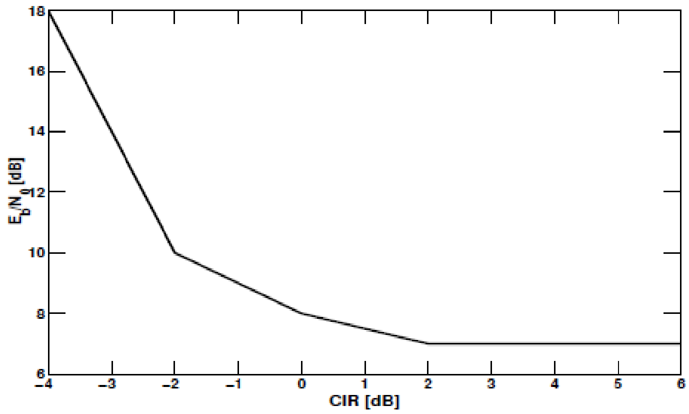

Figure 4. Required E_b/N_0 vs. CIR Before Blind Mode Performance Degrades 30% with Pulse Interferer

CONCLUSTION

In this paper, we present a blind interference cancellation algorithm based on a modification of a previously developed training mode algorithm using the Fractional Fourier Transform (FrFT). The proposed algorithm performs well in non-stationary interference to estimate and cancel interference that could not be cancelled in the time or frequency domains solely, or with MMSE-FrFT methods, which require stationary signals and many samples. We show that even in low carrier-to-interference (CIR) environments, e.g. 0 dB, the proposed blind method performs well, degrading gracefully over the training mode case. Significant degradation occurs only when the CIR is very low, e.g. −2 dB, unless E_b/N_0 is high, or when E_b/N_0 is below about 7 dB. Future work includes testing the blind algorithm on real signals-of-interest (SOIs) and determining how to improve performance at lower E_b/N_0.

ACKNOWLEDGMENT

The author thanks Alan Foonberg at The Aerospace Corporation for reviewing the paper and providing useful suggestions for improvement.

REFERENCES

[1]. Almeida, L.B., "The Fractional Fourier Transform and Time-Frequency Representation", IEEE Trans. on Sig. Proc., Vol. 42, No. 11, Nov. 1994.

[2]. Candan, C., Kutay, M.A., and Ozaktas, H.M., "The Discrete Fractional Fourier Transform", IEEE Trans. on Sig. Proc., Vol. 48, pp. 1329-1337, May 2000.

[3]. Kutay, M.A., Ozaktas, H.M., Arikan, O., and Onural, L., "Optimal Filtering in Fractional Fourier Domains", IEEE Trans. on Sig. Proc., Vol. 45, No. 5, May 1997.

[4]. Kutay, M.A., Ozaktas, H.M., Onural, L., and Arikan, O. "Optimal Filtering in Fractional Fourier Domains", Proc. IEEE Int. Conf. on Acoustics, Speech, and Signal Proc. (ICASSP), Vol. 2, pp. 937-940, 1995.

[5]. O'Toole, J.M., Mesbah, M., and Boashash, B., "Discrete Time and Frequency Wigner-Ville Distribution: Properties and Implementation", Proc. Int. Symposium on Digital Sig. Proc. and Comm. Systems, Noosa Heads, Australia, Dec. 19-21, 2005.

[6]. Ozaktas, H.M., Zalevsky, Z., and Kutay, M.A., "The Fractional Fourier Transform with Applications in Optics and Signal Processing", John Wiley and Sons: West Sussex, England, 2001.

[7]. Subramaniam, S., Ling, B.W., and Georgakis, A., "Filtering in Rotated Time-Frequency Domains with Unknown Noise Statistics", IEEE Trans. on Sig. Proc., Vol. 60, No. 1, Jan. 2012.

[8]. Sud, S., "Estimation of the Optimum Rotational Parameter of the Fractional Fourier Transform Using its Relation to the Wigner Distribution", Int. Journal of Emerging Technology and Advanced Engineering (IJETAE), Vol. 5, No. 9, pp. 77-85, Sep. 2015.